Design and Performance of Alkaline Electrolyzers: An Evolution from HHO to Zero-Gap Systems

Zsolt Čonka

Department of Electrical Energetics, Kandó Kálmán Faculty of Electrical Engineering, Obuda University, Budapest, Hungary
e-mail: conka.zsolt@kvk.uni-obuda.hu

Department of Electric Power Engineering, Faculty of Electrical Engineering and Informatics, Technical University of Košice, Slovakia
e-mail: zsolt.conka@tuke.sk

Abstract: This paper presents a comprehensive study detailing the design evolution and experimental validation of alkaline water electrolyzer's. Progressing from a basic dry-cell HHO generator to an advanced zero-gap system for pure hydrogen production. The initial phase characterized an electrolyzer producing an unstable Brown's gas (HHO). The HHO gas mixture revealed significant limitations related to decreasing efficiency at higher currents and contamination with water vapor. These findings informed the development of a technologically superior alkaline zero-gap electrolyzer. New design implementing porous nickel foam electrodes and a ZIRFON PERL UTP 500 membrane produce high-purity hydrogen separated from oxygen. Experimental validation of this prototype showed that elevating the electrolyte temperature from 20°C to 50°C enhances efficiency from 58.59% to 64.15%. Furthermore, while forced electrolyte circulation improved operational stability, its parasitic energy load reduced overall system efficiency. Finally, long-duration testing confirmed the design's excellent stability, establishing it as a proof-of-concept requiring further optimization for practical implementation.

Keywords: hydrogen; electrolysis; alkaline electrolyzer; HHO gas; Brown's gas; zero-gap

1 Introduction

In the context of the global transition toward sustainable energy systems and the imperative to decarbonize industry and transportation, hydrogen is emerging as a key energy carrier. Its potential lies in its ability to efficiently store surplus electrical energy generated from intermittent renewable sources, such as solar and wind power, and subsequently release it during periods of high demand. The large-scale integration of these variable sources, particularly wind power plants, presents significant challenges to the stability of the electrical grid. Fluctuations in wind speed led to variable power output, which can cause deviations in grid frequency and potentially compromise supply security. Consequently, advanced control strategies, such as regulating the turbine blade pitch angle, are being developed to actively manage power output and provide grid support services [1]. Alongside these control methods, advanced monitoring systems that utilize artificial intelligence for real-time fault detection are becoming critical for maintaining grid resilience and security [2]. This underscores the dual challenge of managing both energy deficits and surpluses. In scenarios of excess generation, energy storage becomes paramount, providing a mechanism to capture otherwise curtailed renewable energy. Water electrolysis is the process of electrochemically splitting water molecules into hydrogen and oxygen using an electric current. It is the foundational technology for producing "green hydrogen," which is considered a cornerstone of the future hydrogen economy [3-5].

This report synthesizes and analyzes the results of evolutionary research focused on the design, construction, and experimental validation of two distinct types of electrolyzer's. The research proceeded in two logically sequential phases, reflecting a progressive increase in complexity and technological maturity:

HHO Generator: The first phase concentrated on the design and testing of a simple alkaline electrolyzer without a separation membrane, which produces a mixture of hydrogen and oxygen in a 2:1 stoichiometric ratio, known as HHO gas or Brown's Gas. This system served as a basic model to verify the principles of electrolysis and to identify key operational challenges and limitations [3, 6].

The Zero-Gap Alkaline Electrolyzer: In the second, more advanced phase, the research focused on the development and detailed analysis of an electrolyzer designed to produce pure, separated hydrogen. This system utilizes the modern "zero-gap" concept, which combines the low material costs of traditional alkaline electrolysis with the high current density and efficiency characteristic of more expensive PEM (Proton Exchange Membrane) electrolyzer's [7-9].

The objective of this report is to provide a comprehensive and critical overview of the entire research process. The report chronologically follows the journey from the initial concept and experiments with the HHO generator, through the analysis of its shortcomings, to the design, structural improvements, and in-depth performance validation of the advanced zero-gap alkaline electrolyzer. Emphasis is placed on the detailed presentation of experimental data, the comparison of measured values with theoretical models, and the identification of key factors influencing the efficiency and stability of both systems [4] [8] [9].

2 Design and Analysis of the HHO Generator

Define The initial phase of the research focused on implementing the basic concept of water electrolysis through the construction and testing of an HHO generator. This approach, while technologically simpler, provided valuable practical experience and revealed fundamental limits that directly motivated the transition to more advanced technologies [7] [9].

2.1 Construction and Operating Principle

The designed HHO generator was based on a "dry-cell" type construction. This system consisted of three parallel-connected series cells, comprising a total of 19 electrodes arranged in an anode-neutral-cathode (– n n n n n + n n n n n – n n n n n +) configuration. A key design feature was the absence of a semi-permeable membrane, meaning that the produced hydrogen and oxygen were not separated and formed a common HHO gas mixture. The electrodes were made of stainless-steel, a material chosen for its corrosion resistance. A 15% aqueous solution of sodium hydroxide (NaOH) served as the electrolyte, acting as a catalyst to reduce the electrical resistance of the water and enable electrolysis at practically achievable voltages. The individual electrodes were mechanically separated by rubber gaskets, which also defined the reaction chambers. The entire assembly of electrodes and gaskets was compressed between two acrylic panels, which served as end plates and contained inlet and outlet ports for the electrolyte and the produced gas. Electrolyte flow into the chambers was ensured by drainage holes at the bottom of the electrodes. HHO gas was extracted through vents at their top. One liter of electrolyte can theoretically generate 1860 liters of HHO gas [3] [9].

Theoretically, the minimum voltage required to start electrolysis between two electrodes is 1.24 V. However, this value is insufficient in practice due to the resistance of the electrolyte solution. The actual minimum voltage depends on the specific electrolyte used; for the NaOH, it is 1.69 V. For comparison, using potassium hydroxide (KOH) would require a minimum of 1.67 V [3] [6].

The complete system, called the HHO generator, included not only the electrolyzer itself but also auxiliary equipment. This included an electrolyte reservoir, which served as a storage tank and foam separator. Gas purifier to remove residual water vapor and impurities and a pressurized vessel to stabilize the gas pressure before its application. System safety was ensured by one-way valves and flashback arrestors designed to prevent a dangerous flame flashback into the generator [3] [6] [10].

2.2 Experimental Measurement of HHO Gas Production

To verify the functionality and quantify the performance of the constructed HHO generator, experimental measurements of gas production were conducted [6]. The measurement methodology was based on the principle of water displacement. The produced HHO gas was directed into a one-liter graduated cylinder, which was submerged and filled with water. As the gas accumulated in the cylinder, it displaced the water. A timer was used to measure the time required to produce one liter of HHO gas. The measures were carried out at various DC supply current values to determine the dependence of gas production on the input electrical power.

The results of two consecutive measurement runs are summarized in the following Tables 1 and 2. The repeated measurement was performed to verify the reproducibility and reliability of the experimental procedure.

Table 1
Performance HHO Gas Production Measurement no. 1

$I_{avg.}$ [A]	U_{source} [V]	***Production time for 1 liter of HHO gas*** **[s]**	V_{HHO} [l/min]
10.1	12.89	82	0.731
15.3	13.32	58	1.03
19.8	13.45	54	1.11
25.2	13.68	42	1.43
29.1	14.54	35	1.714

Table 2
Performance HHO Gas Production Measurement no. 2

$I_{avg.}$ [A]	U_{source} [V]	***Production time for 1 liter of HHO gas*** **[s]**	V_{HHO} [l/min]
10.3	12.89	94	0.638
15.1	12.97	65	0.92
20.1	13.22	44	1.36
25.2	13.44	37	1.62
29.3	16.67	35	1.71

These tables present the primary experimental data that forms the basis for all subsequent analyses. A comparison of the two measurements shows that the results are comparable. The average difference in the production time of one liter of gas is approximately 6 s. This difference could be caused by slight inaccuracies in setting the current, which was not completely constant during the measurement but varied depending on the electrolyte level in the cells. Nevertheless, the data clearly confirms the expected trend: a linear increase in HHO gas production with increasing supply current.

2.3 Comparison with Theoretical Models

A key step in evaluating the electrolyzer's performance is comparing the experimentally obtained data with theoretical predictions. This process not only validates the measurements but also reveals hidden inefficiencies and limitations of the technology used. The first theoretical model was based on Faraday's laws of electrolysis, which allow for the calculation of the theoretical volume of hydrogen (V_{H}) produced based on the total electric charge passed through the cell:

$$V_{\mathrm{H}} = \frac{R \cdot T \cdot Q}{F \cdot p \cdot z_{\mathrm{H}}} \, [\mathrm{l/min}] \tag{1}$$

where: R – universal gas constant, T – temperature, Q – total electric charge, F – Faraday constant, p – pressure, z_{H} – number of excess electrons for hydrogen.

Table 3

Comparison of Measured and Calculated HHO Gas Production (Faraday's Law) [3] [6]

$I_{avg.}$ [A]	$V_{meas.HHO}$ [l/min]	$V_{pred.HHO}$ [l/min]	Δ_{rel} [%]
10	0.731	0.336	54.04
15	1.03	0.504	51.07
20	1.11	0.675	39.19
25	1.43	0.841	41.15
29	1.714	1.008	41.19

The data in Table 3 reveal a massive and systematic discrepancy between theory and experiment. The measured production values are consistently 39% to 54% higher than predicted. Its cause lies in the very nature of the HHO generator, and the measurement method used. Higher current causes significant heating of the electrolyte, which leads to the evaporation of water and the generation of a significant amount of water vapor. The measurement method of water displacement measures the total volume of all gaseous components, including water vapor. The "measured production" is thus artificially inflated by the volume of this vapor, which does not contribute energetically to the value of HHO as a fuel. To obtain a more accurate theoretical estimate, the freely available software "HHO Hydrogen Generator Cell Configurator" was used. This part includes the data on the measuring method and instruments as well as experimental results.

The results from following Table 4 show a significantly better agreement, confirming that a more advanced model that considers the geometry and construction of the cell provides more realistic predictions.

Table 4

Comparison of Measured and Software Calculated HHO Gas Production [3] [6]

$I_{avg.}$ [A]	$V_{meas.HHO}$ [l/min]	$V_{pred.HHO}$ [l/min]	Δ_{rel} [%]
10	0.731	0.626	14.36
15	1.03	0.94	8.74

$I_{avg.}$ [A]	$V_{meas.HHO}$ [l/min]	$V_{pred.HHO}$ [l/min]	Δ_{rel} [%]
20	1.11	1.25	-12.61
25	1.429	1.565	-9.52
29	1.714	1.879	-9.63

2.4 Efficiency, Losses, and Practical Application

Overall energy efficiency is a key parameter for evaluating any energy device. The efficiency (η) of the HHO generator was calculated as the ratio of the chemical energy contained in the produced hydrogen to the supplied electrical energy, using the following formula [3] [6] [9]:

$$\eta = \frac{n \cdot \Delta H \cdot V}{U \cdot I \cdot t} \cdot 100\ [\%] \tag{2}$$

where: n – number of moles of hydrogen, ΔH – enthalpy of combustion for hydrogen, V – measured volume of gas produced, U, I, and t represent the voltage, current, and time of the supplied electrical energy, respectively.

Table 5

HHO Generator Efficiency

$I_{avg.}$ [A]	U_{source} [V]	V_{HHO} (no. 1) [l/min]	η [%]
10.1	12.89	0.731	86.668
15.3	13.32	1.03	78.118
19.8	13.45	1.11	64.424
25.2	13.68	1.429	64.07
29.1	14.54	1.714	62.613

The data in Table 5 reveal an important trend: as the current gas production increases, the efficiency of the electrolyzer significantly decreases, from nearly 87% to approximately 63%. This decline is a direct consequence of increasing losses in the system, primarily Joule heating, overpotential gas bubbles, and chemical losses from electrode degradation. The practical application of HHO gas was tested by burning it in a gas torch. The total power was estimated to be only 60 to 70 W, which, compared to the input electrical power of up to 423 W, demonstrates extremely low overall efficiency.

3 Advanced Zero-Gap Alkaline Electrolyzer

Based on the knowledge and limitations identified in the first phase of research, the second phase focused on the development of a substantially more advanced system. The main goal was to overcome the shortcomings of the HHO generator by transitioning to an alkaline electrolyzer with a membrane, which produces separated hydrogen [7-9].

3.1 Theoretical Concept and Motivation for Change

The primary motivation for changing the technological approach was the need to produce pure hydrogen, which is significantly more stable and versatile than the explosive HHO mixture. To achieve high efficiency, an innovative "zero-gap" design was chosen. The principle involves minimizing the distance between the anode and cathode to the thickness of the separation membrane itself. This dramatically reduces the ohmic resistance of the electrolyte, which is one of the main sources of loss in traditional alkaline electrolyzer’s. This approach allows for high current densities and efficiency while maintaining low material costs. By adopting this principle, the system can achieve current densities significantly higher than the typical 0.25 $A \cdot cm^{-2}$ of traditional alkaline electrolyzer’s, approaching the 2 $A \cdot cm^{-2}$ characteristic of more expensive PEM systems [4, 7-9, 13].

3.2 Key Components and Materials

The success of the zero-gap concept is directly dependent on the correct choice of materials for the key components: the electrodes and the membrane. The electrolyte was also updated from the previously used NaOH to a 30% aqueous solution of KOH, which is common in high-performance alkaline systems [8].

The new design utilizes electrodes made of porous nickel foam with a porosity of 75 PPI (pores per inch). This choice offered two fundamental advantages. First, nickel is highly resistant to corrosion in an alkaline environment and does not release undesirable oxides, eliminating contamination and extending the device's lifespan. Second, the highly porous structure provides an extremely large active surface area for electrochemical reactions, which is crucial for achieving high current densities [8] [14].

The central element of the electrolyzer is the ZIRFON PERL UTP 500 composite membrane. It is composed of a polyphenylene sulphide fabric coated with a mixture of a polymer and zirconium dioxide, giving it mechanical strength and chemical stability up to 110 °C. A key property of this membrane is its ionic resistance, which significantly decreases with increasing electrolyte temperature, making operation at higher temperatures energetically more favorable [7-9, 15].

The careful selection of these advanced materials for electrodes, membrane, and electrolyte is central to the electrolyzer’s performance. This focus on material science is reflective of a wider trend in electrical engineering, where enhancing the properties of functional liquids is a key area of research. For instance, recent studies on insulating oils for high-voltage equipment have demonstrated that suspending hybrid nanoparticles, such as magnetite (Fe_3O_4) and fullerene (C_{60}), can significantly alter a liquid's dielectric and thermal properties. While the objective of such nanofluids is to improve insulation, and electrolytes aim to maximize ionic conductivity, both fields rely on engineering liquids at the nanoscale to achieve superior performance in electrical systems [16].

3.3 Design Challenges and the Final Model

After The transition from a theoretical concept to a functional device was an iterative process. The first prototype suffered from electrolyte leakage and an unreliable electrical supply to the electrodes. The sealing problem was solved by adjusting the bolt layout based on the successful mechanical design of the HHO generator. The power supply issue was resolved by modifying the quick-connect fittings to serve a dual function as both hydraulic connections and reliable, low-resistance electrical contacts. The result was a final, functional, and reliable electrolyzer model, ready for detailed experimental testing [7-9, 17].

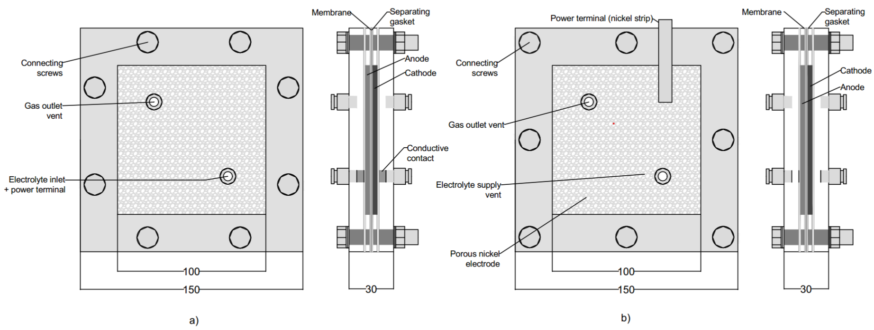

Figure 1

(a) Final version of the functional electrolyzer, (b) Prototype electrolyzer [5, 6]

4 Experimental Validation and Performance Analysis of the Zero-Gap Electrolyzer

Following the successful construction of the final zero-gap electrolyzer model, a series of laboratory measurements were conducted to quantify its performance and verify theoretical assumptions. The experimental program systematically investigated the influence of electrolyte temperature, forced circulation, and long-term operation [4-6].

4.1 Analytical Methods

The performance analysis of the zero-gap electrolyzer involved comparing experimentally measured values with theoretically calculated ones. The relative difference (Δ_{rel}) between the measured ($V_{meas.}$) and calculated ($V_{calc.}$) hydrogen production was determined using the formula [7-9]:

$$\Delta_{rel} = \frac{V_{meas.} - V_{calc.}}{\frac{V_{meas.} + V_{calc.}}{2}} \cdot 100\% \ [\%] \quad (3)$$

4.2 Initial Functional Tests and Commissioning

Before taking measurements, the assembled electrolyzer passed several functional tests to ensure it was working correctly. The first major challenge was preparing the electrolyte, as the process generated significant heat and required careful handling with safety equipment. [8] [9].

After filling the system, minor leaks were observed around the bolts and threads. These were successfully resolved by carefully tightening the connections and applying rubber O-rings to ensure a perfect seal. A more significant issue arose during the initial power-on test, where an unusually high production of oxygen was observed, suggesting faulty electrical contact on the anode side. An investigation confirmed the presence of high transitional resistance at the connection point, which was causing localized overheating and degradation of the nickel foam electrode. The problem was solved by welding the threaded connection and introducing a nickel strip to expand the contact area with the electrode, which stabilized gas production. A final qualitative test, involving the ignition of the output gas streams, confirmed the proper functioning of the separation membrane: the gas from the cathode side produced the characteristic sound of hydrogen ignition, while the oxygen from the anode side showed no reaction [3, 7-9].

4.3 Experimental Measurement 1: Influence of Electrolyte Temperature

The first quantitative experiment focused on the effect of electrolyte temperature on the electrolyzer's production rate and efficiency. The methodology involved comparing the system's performance at two distinct operating temperatures: room temperature (approximately 20°C) and elevated temperature (approximately 50 °C). The detailed measurements of hydrogen production at both temperatures are presented in Tables 6 and 7, while the resulting efficiency calculations are summarized in Tables 8 and 9. This relationship is also visualized in Fig. 2, which plots the linear increase in hydrogen production with rising source current for both temperature settings [8] [9] [18].

Table 6

Hydrogen Production Measurement at $\vartheta \approx 20$ °C and $U_{source} = 2.5$ V [3] [6]

$I_{avg.}$ [A]	$V_{avg.}$ [l/min]	$V_{calc.}$ [l/min]	*Energy Cons.* [J]	Δ_{rel} [%]
2.33	0.0171	0.0174	204.4	1.89
2.32	0.0169	0.0174	205.9	2.64
2.34	0.0174	0.0175	201.7	0.58
2.33	0.0171	0.0174	204.4	1.89
2.35	0.0177	0.0176	199.2	0.71

Table 7

Hydrogen Production Measurement at $\vartheta \approx 50$ °C and $U_{source} = 2.4$ V [3] [6]

$I_{avg.}$ [A]	$V_{avg.}$ [l/min]	$V_{calc.}$ [l/min]	*Energy Cons.* [J]	Δ_{rel} [%]
2.38	0.0179	0.0196	191.5	9.18
2.52	0.0198	0.0208	183.3	4.81
2.47	0.0195	0.0204	182.4	4.33
2.47	0.0195	0.0204	182.4	4.33
2.55	0.0195	0.0210	188.3	7.52

Table 8

Theoretical Efficiency Calculation without Forced Circulation at $\vartheta \approx 20$°C [3] [6]

$I_{avg.}$ [A]	U_{source} [V]	$V_{avg.\ measured}$ [l/min]	η [%]
1.26	2.2	0.0076	54.37
1.614	2.3	0.0098	52.34
1.96	2.4	0.013	54.63
2.334	2.5	0.0172	58.59

Table 9

Theoretical Efficiency Calculation without Forced Circulation at $\vartheta \approx 50$°C [3] [6]

$I_{avg.}$ [A]	U_{source} [V]	$V_{avg.\ measured}$ [l/min]	η [%]
1.202	2.2	0.0078	58.34
2.338	2.3	0.0174	62.86
2.487	2.4	0.0192	64.15

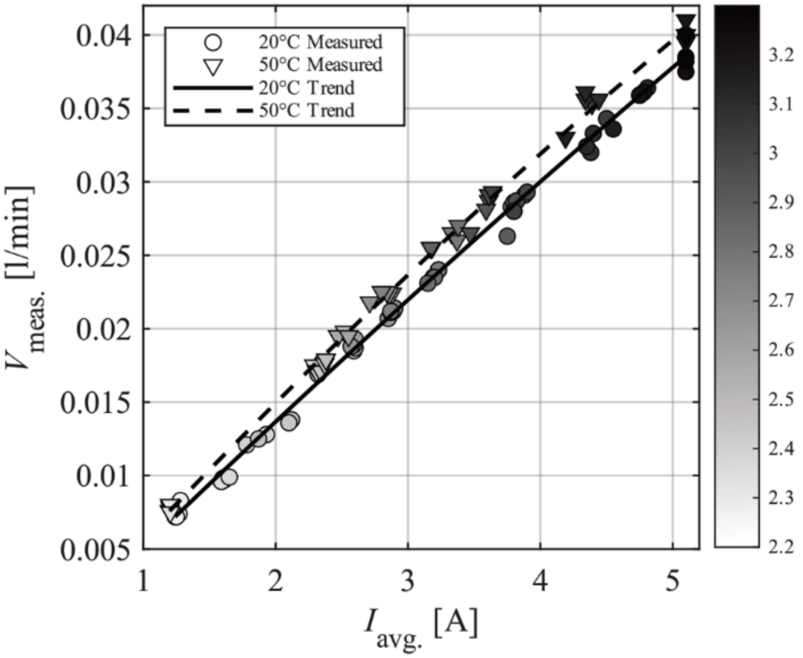

Figure 2

Comparison of voltage dependence of measured volume at temperatures of $\vartheta \approx 20$ °C and 50 °C [5][6]

The data in these tables clearly confirms the significant positive impact of preheating the electrolyte. The onset of the electrolytic reaction was observed at approximately 1.49 V, closely matching the calculated thermoneutral voltage of 1.48 V for alkaline electrolysis. As shown in Table 9, at an operating source voltage of 2.4 V with the heated electrolyte, the system achieved an efficiency of 64.15%. In contrast, with the cold electrolyte (Table 8), a higher source voltage of 2.5 V was required to achieve a lower efficiency of 58.59%. This demonstrates that preheating the electrolyte is a highly effective way to increase production and efficiency, as it lowers the internal resistance of the system [8] [9].

4.4 Experimental Measurement 2: Influence of Forced Electrolyte Circulation

This experiment was designed to assess impact of introducing a forced flow of the electrolyte using external pumps. The measurement was conducted at a stable temperature (20 °C) and a constant electrolyzer voltage ($U_z = 2.5$ V), while voltage applied to the circulation pumps varied across eleven levels from 0.9 V to 3 V. The results, showing the cell efficiency (η_{cell}) versus the total system efficiency (η) at various pump voltages, are detailed in Table 10 and visualized in Fig. 3 [8] [9].

Table 10
Hydrogen Cell efficiency (η_{cell}) and total system efficiency (η) of the zero-gap electrolyzer with forced circulation at 20 °C and a source voltage of 2.5 V [3] [6]

$I_{avg.}$ [A]	$V_{avg. measured}$ [l/min]	η_{cell} [%]	η [%]	***Energy Cons.*** [J]
2.317	0.01746	59.77	34.93	217.48
2.325	0.01794	61.2	34.44	217.74
2.33	0.01848	62.91	34.39	211.41
2.33	0.0184	62.64	33.29	215.54
2.335	0.01796	61.01	31.33	223.61
2.335	0.01842	62.57	30.91	222.12
2.34	0.01806	61.22	28.47	231.42
2.35	0.01816	61.29	26.17	240.72
2.355	0.0183	61.64	24.18	248.13
2.36	0.0186	62.51	22.09	269.34
2.36	0.01866	62.72	19.36	297.96

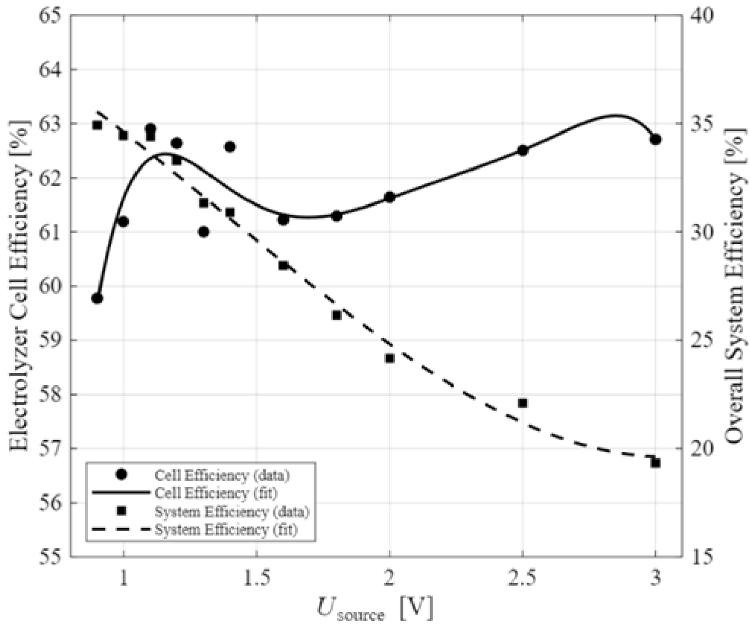

Figure 3
Impact of forced circulation on the efficiency of the electrochemical cell versus the total system [5, 6]

The results revealed an important "efficiency paradox". The forced circulation did lead to a more stable current draw and a slight increase in the efficiency of the electrochemical cell itself (η_{cell}), which peaked at 62.91%. However, this gain was completely overshadowed by the energy consumed by the pumps. When this parasitic load was included, the overall system efficiency (η) dropped dramatically to a maximum of just 34.39%. From a purely energetic standpoint, forced circulation proved to be inefficient, though it offered operational benefits like ensuring a smoother, more continuous evolution of hydrogen gas [7-9, 19].

4.5 Experimental Measurement 3: Long-Term Operational Stability

The final experiment aimed at analyzing the electrolyzer's performance and stability during prolonged, continuous operation, simulating real-world usage. The test was conducted under the optimal conditions for stability identified previously: a source voltage of 2.5 V and a circulation pump voltage of 1.1 V. The evolution of the key operational parameters is presented in Fig. 4 [8].

The analysis confirmed the excellent self-regulating capability and stability of the device. During the first two hours of operation, the system reached a thermal and electrical steady state. The electrolyte temperature, as shown in Fig. 4b, rose by a modest 1.4 °C before stabilizing at around 21.1 °C. The current drawer (Fig. 4a) closely followed this temperature profile, rising initially before settling at a consistent 2.355 A. This behavior was attributed to rising electrolyte temperature, which increased its conductivity from an initial ≈7.61 $S \cdot m^2/mol$ to ≈8.4 $S \cdot m^2/mol$, thereby reducing the energy consumption per unit of gas produced [7] [9]. The hydrogen production rate (Fig. 4c) mirrored these trends, also achieving a stable output. The average efficiency was stable across both measurement runs, reaching 33.09% during measurement no. 1 and 32.88% during measurement no. 2, confirming consistent performance over time. Ultimately, the electrolyzer operated continuously without any signs of performance degradation or physical damage, proving it is technically capable of long-term, steady-state operation [3, 8, 9].

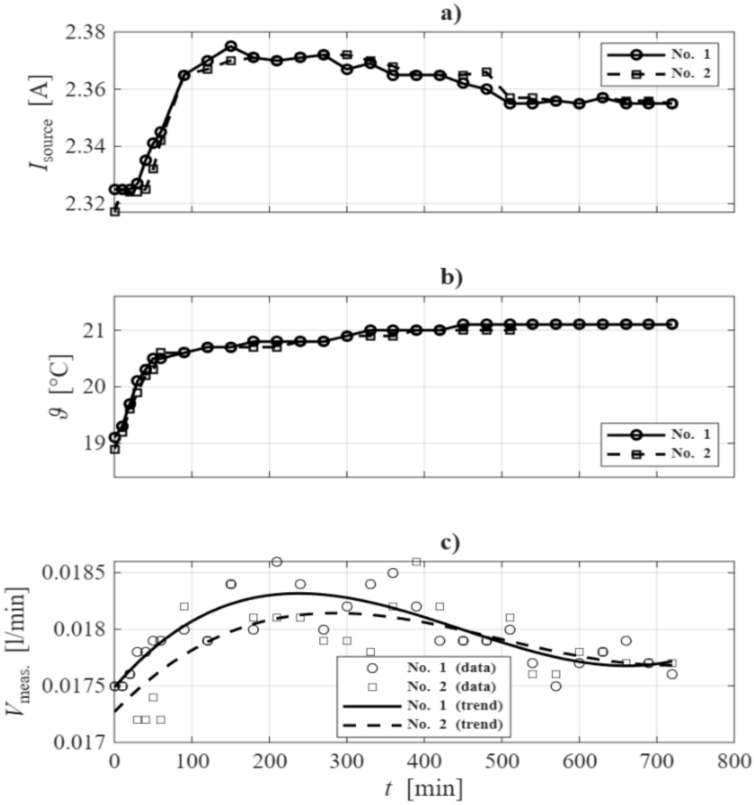

Figure 4

Evolution of key electrolyzer parameters as a function of operating time: (a) source current draw, (b) electrolyzer temperature, and (c) hydrogen production rate [8, 9]

5 Future Outlook

This research successfully documented the complete evolutionary cycle of designing, constructing, and testing two distinct generations of alkaline water electrolyzer’s. The work progressed logically from a foundational "dry-cell" HHO generator, designed to explore the basic principles of electrolysis, to a technologically advanced zero-gap alkaline electrolyzer aimed at producing pure, separated hydrogen gas. This two-phase approach allowed for the identification of critical limitations in simpler designs, which directly informed the development of the superior final prototype. The research culminated in the successful validation of this advanced model, confirming its stability, efficiency, and suitability for further scientific investigation.

5.1 Key Findings and Performance of the Zero-Gap Electrolyzer

The research led to the successful construction and validation of a functional zero-gap alkaline electrolyzer, whose performance was rigorously quantified through a series of experiments. The key findings are summarized as follows:

Temperature influence: Experimental measurements confirmed that preheating the electrolyte is a highly effective method for boosting performance. Increasing the electrolyte temperature from approximately 20 °C to 50 °C resulted in a significant rise in energy efficiency from 58.59% to 64.15%, primarily due to the reduction of the electrolyte's ohmic resistance.

Forced circulation paradox: The analysis of forced electrolyte circulation revealed a critical trade-off between operational stability and overall energy efficiency. While circulation did improve the stability of the system, the parasitic energy consumption of the pumps drastically reduced the total system efficiency, with a peak value of only 34.39%. This suggests that for this specific configuration, the energy cost of pumping outweighs the electrochemical benefits.

Long-term stability: Long-duration tests confirmed the robustness and excellent self-regulating capability of the final model. The electrolyzer achieved a stable thermal and electrical regime after an initial warm-up period and operated continuously for over 12 hours without any signs of performance degradation, proving its technical suitability for prolonged operation.

5.2 Comparative Analysis of Electrolyzer Technologies

The technological progress achieved is most evident when comparing the performance and characteristics of the initial HHO generator with the final zero-gap model. The HHO generator produced an unstable and difficult-to-use mixture of hydrogen and oxygen, which was further contaminated with significant amounts of water vapor and metal oxides (like chromium oxides from the stainless-steel electrodes). In stark contrast, the zero-gap electrolyzer, equipped with a ZIRFON membrane and nickel foam electrodes, produced pure, separated hydrogen ready for further use. Furthermore, the HHO generator exhibited significant thermal instability and a lower efficiency that sharply decreased under increasing load (from nearly 87% at low current to 63% at high current). The zero-gap model demonstrated excellent thermal stability and achieved a higher, more consistent efficiency. Finally, the behavior of the HHO generator deviated significantly from theoretical predictions, whereas the zero-gap model showed excellent agreement between experimental data and theoretical calculations, allowing for its reliable characterization.

5.3 Outlook and Recommendations for Further Research

The results of this research establish the constructed zero-gap electrolyzer as a successful proof-of-concept and a valuable platform for future investigations. A key direction for these future efforts lies in demonstrating the electrolyzer's role within the context of modern, decentralized power systems. The electrical grid is increasingly evolving into a network of microgrids, which are localized energy systems designed to manage various distributed energy resources (DERs) and require advanced electrical protection schemes to ensure stability and security. Therefore, a critical next step for this research would be to integrate the validated electrolyzer into a microgrid testbed. This would allow for the practical evaluation of its performance as a controllable DER, capable of providing grid-balancing services and enhancing the overall resilience that these next-generation energy systems demand.

A further avenue for application-focused research is to demonstrate the synergy between this electrolyzer and advanced hydrogen conversion technologies. For instance, low-temperature solid oxide fuel cells (SOFCs) are highly efficient devices for generating electricity from hydrogen but often produce low-voltage power at reduced operating temperatures, necessitating the use of DC-DC voltage boosters to deliver usable power. Coupling the validated zero-gap electrolyzer with an LT-SOFC system would create a complete green hydrogen production-to-power demonstration, validating the practical utility of the high-purity hydrogen generated by the device.

However, a more promising path lies in improving the electrochemical performance of the reaction cell itself. As indicated in the design phase, the next logical step is the application of low-cost, highly active catalysts to the surface of the porous nickel electrodes. The use of Ni/Fe alloys, applied through methods like electrodeposition, has the potential to significantly reduce the reaction overpotential. This would allow the electrolyzer to operate at higher current densities with lower voltage requirements, thereby substantially increasing the overall energy efficiency and the economic attractiveness of this technology for practical hydrogen production.

To accelerate this optimization process, future work could also incorporate data-driven computational methods. For instance, machine learning (ML) models are increasingly used to predict the performance of clean energy devices and guide experimental efforts, as demonstrated in the optimization of dye-sensitized solar cells (DSSCs) where ML can identify key manufacturing parameters that most influence efficiency. A similar approach could be developed for the zero-gap electrolyzer, creating a predictive model based on parameters such as catalyst composition, electrode morphology, and operating conditions. This would allow for a more strategic and efficient exploration of the vast parameter space, focusing laboratory work on the most promising configurations.

Acknowledgements

This research was funded by the Slovak Ministry of Education, Science, Research and Sport of the Slovak Republic and the Slovak Academy of Sciences VEGA 1/0627/24.

References

[1] Z. Conka, L. Bena, R. Stefko, M. Pavlik, P. Holcsik, and J. Palfi, 'Wind Turbine Power Control According to EU Legislation', *Energies*, Vol. 15, No. 22, p. 8614, Nov. 2022, doi: 10.3390/en15228614

[2] M. Bobček, Z. Čonka, and J. Palfy, 'Neural Network-Based Fault Learning Using Artificial Intelligence and Kalman's Filter', in *2024 IEEE 18th International Symposium on Applied Computational Intelligence and Informatics (SACI)*, May 2024, pp. 000389-000394, doi: 10.1109/SACI60582.2024.10619813

[3] V. Szomosi, 'Possibilities of using an electrolyzer for electricity generation purposes', Technical University of Košice, 2023, Accessed: May 22, 2024, https://opac.crzp.sk/?fn=docview2ChildA1SDG&record=C03CB0FBA6588971DC3921D1B6BF&seo=CRZP-Prehliadanie-pr%C3%A1c

[4] J. Balajka, *Hydrogen and other new energy carriers*. in Energy Literature Edition. Bratislava: Alfa, 1982

[5] E. López-Fernández, C. G. Sacedón, J. Gil-Rostra, F. Yubero, A. R. González-Elipe, and A. de Lucas-Consuegra, 'Recent Advances in Alkaline Exchange Membrane Water Electrolysis and Electrode Manufacturing', *Molecules*, Vol. 26, No. 21, p. 6326, Jan. 2021, doi: 10.3390/molecules26216326

[6] V. Szomosi and D. Medveď, 'Possibilities of using an electrolyzer for electricity generation purposes', in *Electrical Engineering and Informatics*, in 14, No. 14, Faculty of Electrical Engineering and Informatics Technical University of Košice Letná 9, 040 01 Košice, Slovak Republic, p. 486, Available: https://eei.fei.tuke.sk/wp-content/uploads/2024/03/EEI_14.pdf

[7] V. Szomosi and D. Medveď, 'Design of a hydrogen production facility', in *Electrical Engineering and Informatics*, in 15, No. 15, Faculty of Electrical Engineering and Informatics Technical University of Košice Letná 9, 040 01 Košice, Slovak Republic, p. 524, Available: https://eei.fei.tuke.sk/wp-content/uploads/2024/07/EEI_15.pdf

[8] V. Szomosi and D. Medveď, 'Design of a hydrogen production facility II', in *Electrical Engineering and Informatics*, in 16, No. 16, Faculty of Electrical Engineering and Informatics Technical University of Košice Letná 9, 040 01 Košice, Slovak Republic, p. 658, Available: https://eei.fei.tuke.sk/wp-content/uploads/2025/07/EEI_16.pdf

[9] V. Szomosi, ‘Design of a hydrogen production facility’, Diploma thesis, Technical University of Košice. https://opac.crzp.sk/?fn=detailBiblioFormChildY1FKM0&sid=AF7DAECCF8461446C79041FD86FE&seo=CRZP-detail-kniha

[10] A. K. El Soly, M. A. El Kady, A. E. F. Farrag, and M. S. Gad, ‘Comparative experimental investigation of oxyhydrogen (HHO) production rate using dry and wet cells’, *Int. J. Hydrog. Energy*, Vol. 46, No. 24, pp. 12639-12653, Apr. 2021, doi: 10.1016/j.ijhydene.2021.01.110

[11] D. Biggs, ‘Cell Configurator’. Accessed: Mar. 08, 2023 [Online] Available: http://www.hho4free.com/configurator/cell_configurator.html

[12] Q. Li *et al.*, ‘Anion Exchange Membrane Water Electrolysis: The Future of Green Hydrogen’, *J. Phys. Chem. C*, Vol. 127, Mar. 2023, doi: 10.1021/acs.jpcc.3c00319

[13] M. Klingenhof *et al.*, ‘High-performance anion-exchange membrane water electrolysers using NiX (X = Fe,Co,Mn) catalyst-coated membranes with redox-active Ni–O ligands’, *Nat. Catal.*, Vol. 7, pp. 1213-1222, Oct. 2024, doi: 10.1038/s41929-024-01238-w

[14] A. L. Santos, M. J. Cebola, J. Antunes, and D. M. F. Santos, ‘Insights on the Performance of Nickel Foam and Stainless Steel Foam Electrodes for Alkaline Water Electrolysis’, *Sustainability*, Vol. 15, No. 14, p. 11011, Jan. 2023, doi: 10.3390/su151411011

[15] Agfa-Gevaert NV, ‘ZIRFON PERL UTP 500’. Accessed: May 22, 2024 [Online] Available: https://www.agfa.com/specialty-products/wp-content/uploads/sites/8/2020/06/TDS_ZIRFON_PERL_UTP_500_20200525.pdf

[16] P. Havran *et al.*, ‘Dielectric relaxation spectroscopy of hybrid insulating nanofluids in time, distribution, and frequency domain’, *J. Mol. Liq.*, Vol. 409, p. 125409, Sept. 2024, doi: 10.1016/j.molliq.2024.125409

[17] V. Kumar and A. K. Tiwari, ‘Design implication of alkaline water electrolyzer for green hydrogen generation towards efficiency, sustainability, and economic viability’, *Int. J. Hydrog. Energy*, Vol. 100, pp. 201-213, Jan. 2025, doi: 10.1016/j.ijhydene.2024.12.294

[18] R. Phillips and C. Dunnill, ‘Zero Gap Cell Design for Alkaline Electrolysis’, 2019. doi: 10.13140/RG.2.2.26663.29606

[19] L. Deng *et al.*, ‘Bubble evolution dynamics in alkaline water electrolysis’, *eScience*, Vol. 5, No. 4, p. 100353, July 2025, doi: 10.1016/j.esci.2024.100353

[20] M. Bobcek, R. Stefko, and Z. Conka, ‘Electrical Protection Systems for the Evolving Microgrid Environment’, *Acta Polytech. Hung.*, Vol. 20, No. 11, pp. 159-178, 2023, doi: 10.12700/APH.20.11.2023.11.10

[21] M. U. Rahman *et al.*, 'Electrochemical investigation of bismuth-doped anode materials for low-temperature solid oxide fuel cells with boosted voltage using a DC-DC voltage converter', *Nanotechnol. Rev.*, Vol. 14, No. 1, Jan. 2025, doi: 10.1515/ntrev-2025-0148

[22] 'NiFe-LDH as a bifunctional electrocatalyst for efficient water and seawater electrolysis: enhanced oxygen evolution and hydrogen evolution reactions', *Nanoscale Adv.*, Vol. 7, No. 18, pp. 5546-5560, July 2025, doi: 10.1039/d5na00350d

[23] X. He, X. Wang, and H. Xu, 'Advancements in Cobalt-Based Catalysts for Enhanced CO2 Hydrogenation: Mechanisms, Applications, and Future Directions: A Short Review', *Catalysts*, Vol. 14, No. 9, p. 560, Sept. 2024, doi: 10.3390/catal14090560

[24] Z. Varga, M. Bobcek, Z. Conka, and E. Racz, 'Machine Learning-Based Prediction of Dye-Sensitized Solar Cell Efficiency for Manufacturing Process Optimization', *Energies*, Vol. 18, No. 18, p. 5011, Jan. 2025, doi: 10.3390/en18185011

[25] Nikolaos Koltsaklis, Jaroslav Knápek, "The Role of Flexibility Resources in the Energy Transition", *Acta Polytechnica Hungarica*, Vol. 20, No. 11, 2023, DOI: 10.12700/APH.20.11.2023.11.9

[26] Diahovchenko I. et. al., "Demand-Supply Balancing in Energy Systems with High Photovoltaic Penetration, using Flexibility of Nuclear Power Plants", *Acta Polytechnica Hungarica*, Vol. 20, No. 11, 2023, DOI:10.12700/APH.20.11.2023.11.8

[27] Javed MY et.al., "Improving the efficiency of photovoltaic-thermoelectric generator system using novel flying squirrel search optimization algorithm: Hybrid renewable and thermal energy system (RTES) for electricity generation", Process safety and environmental protection, Vol. 187, pp. 104-116, 2024, DOI 10.1016/j.psep.2024.04.093

[28] Pavlík M. et.al., "Analysis and Evaluation of Photovoltaic Cell Defects and Their Impact on Electricity Generation", *Energies*, Vol. 16, Issue: 6, 2023, DOI: 10.3390/en16062576